

10f1

A QUANTITATIVE MODEL FOR INTERPRETING NANOMETER SCALE HARDNESS MEASUREMENTS OF THIN FILMS, W.H. Poisl and B.D. Fabes, Department of Materials Science and Engineering, University of Arizona, Tucson, AZ 85721, and W.C. Oliver, Metals and Ceramics Division, Oak Ridge National Laboratories, Oak Ridge, TN, 37831.

Abstract

A model has been developed to determine the hardness of thin films from hardness versus depth curves, given the thickness of the film and hardness of the substrate. The model is developed by dividing the measured hardness into film and substrate contributions based on the projected areas of both the film and substrate under the indenter. The model incorporates constraints on the deformation of the film by the surrounding material in the film, the substrate, and friction at the indenter/film and film/substrate interfaces. These constraints increase the pressure that the film can withstand and account for the increase in measured hardness as the indenter approaches the substrate.

The model is evaluated by fitting the predicted hardness versus depth curves obtained from titanium and Ta_2O_5 films of varying thicknesses on sapphire substrates. The model is also able to describe experimental data for Ta_2O_5 films on sapphire with a carbon layer between the film and the substrate by a reduction in the interfacial strength from that obtained for a film without an interfacial carbon layer.

Introduction

Depth-sensing indentation instruments have been used to determine the mechanical properties, especially Young's modulus, E , and hardness, H , of thin films and coatings on the nanometer scale. In measuring the hardness of a thin film, it is often observed that, for the same depth of penetration, hardness increases as the thickness of the film decreases. It has been difficult to separate the individual mechanical properties of the film and substrate from the measured composite properties of the film/substrate system. The interactions between the intrinsic (dislocation density, crystal structure, etc.) and extrinsic (substrate hardness, film/substrate adhesion, film thickness, etc.) properties on the measured hardness are not well understood.

If a soft film adheres to a hard substrate, or if there is friction between the film and substrate, the substrate will constrain the plastic flow of the film. This will induce a hydrostatic pressure under the indenter, making penetration by the indenter more difficult. As the hardness of the system is defined as the maximum load divided by the projected permanent area of the indent, this will cause an increase in hardness as the indenter approaches the substrate. For films of the same thickness, an increase in friction between the film and substrate should result in a higher hardness for the same depth of penetration. This has been observed for aluminum films on silicon with and without a carbon layer on the substrate.⁶ The level of friction can range from the case where there is perfect sliding, to the case where there is perfect adhesion between the film and substrate. This can be considered to be a case of "sticking friction", where the coefficient of friction is high enough to prevent material from sliding past one another.

Various models of the indentation process have been proposed to obtain the expected hardness versus depth curves. These have included finite element models,¹ as well as physical models based on weighted volumes^{2,4} or areas^{3,6} of material affected by the indenter. Many of these models, however, have not used the actual area function of the

The submitted manuscript has been authorized by a contractor of the U.S. Government under contract No. DE-AC06-84OR21400. Accordingly, the U.S. Government retains a nonexclusive, royalty-free license to publish or reproduce the published form of this contribution, or allow others to do so, for U.S. Government purposes.

indenter, have not included the full range of indentation depths (both less than and greater than the film thickness), or included changes in film/substrate adhesion.

In this paper a physical model based on the areas of film and substrate under the indenter, along with constraints imposed by the adhesion of the film to the substrate, is developed. From this model an equation is developed that relates the measured hardness to the intrinsic hardness of the film, knowing the thickness of the film and hardness of the substrate. The equation is evaluated by fitting it to the experimentally determined hardness versus depth curves.

Development of Model

In the development of this model, the film hardness is considered to be an intrinsic property which is modified by constraints, which cause an increase in measured hardness as indentation proceeds. There are two interrelated aspects to the constraint: friction at the interfaces and the distribution of stress within the film. As indentation proceeds, a compressive, hydrostatic pressure is produced in the film between the substrate and the indenter. This pressure will depend on the friction (or the shear strength) at the indenter/film and film/substrate interfaces, as well as the depth of penetration. For a given depth of penetration, an increase in interfacial shear strength will result in an increase in the hydrostatic pressure, producing an increase in measured hardness. For a given interfacial shear strength, the hydrostatic pressure will increase as the depth of penetration increases, producing an increase in the measured hardness.

The constraint can be analyzed by utilizing a model for the forging of a cylindrical specimen between two flat, rigid dies under frictional conditions. Using an analysis based on the Von Mises yield criterion and a constant coefficient of Coulomb friction, μ , an equation for the pressure under the indenter, p , as a function of radius, r , from the center of the indenter can be obtained by balancing the forces on an element in equilibrium.⁷

$$\left(\frac{p}{\sigma_0}\right) = e^{2\mu\left(\frac{r_0-r}{h}\right)} \quad (1)$$

Here r_0 is the radius of the indent, h is the distance from the indenter to the substrate and σ_0 is the yield strength of the film.

If, instead of a constant coefficient of friction, the interface can be described as having a constant shear strength, τ , and using the sticking friction condition that $\tau = \sigma_0/\sqrt{3}$, the following equation can be obtained:

$$\left(\frac{p}{\sigma_0}\right) = 1 + \frac{2}{\sqrt{3}} \left[\frac{r_0 - r}{h} \right] \quad (2)$$

The pressure distribution is symmetric about the center of the disk, rising from a value of σ_0 at the perimeter of the disk to a sharp peak at the center. This increase in pressure with distance is often called a friction hill⁷, and is shown in Figure 1.

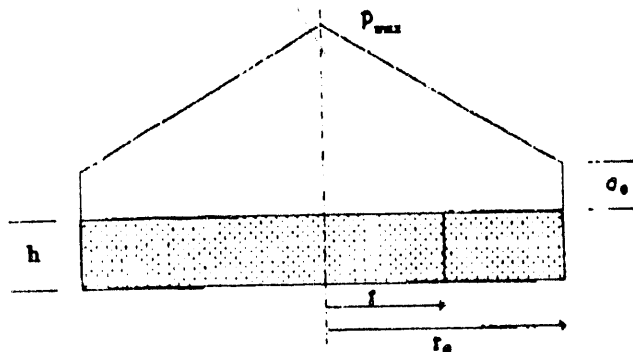


Figure 1. Distribution of stress in a circular disk for homogeneous compression with sticking friction.

If the interfacial shear strength is some constant fraction of the yield strength in shear, the above equation can be modified to include an interfacial friction factor, m (also known as Tresca's friction factor), as follows:

$$\left(\frac{p}{\sigma_0} \right) = 1 + \frac{2m}{\sqrt{3}} \left(\frac{r_o - r}{h} \right) \quad (3)$$

where m can vary from 0 (perfect sliding) to 1 (sticking friction).

By multiplying the film hardness, H_f , by the constraint, the measured hardness, H_m , can be obtained as follows:

$$H_m = H_f \left(1 + \beta \frac{r_o - r}{h} \right) \quad (4)$$

where β replaces the $(2m/\sqrt{3})$ term in equation 3.

This type of approach has been used by Stone *et al.*⁶ to model the indentation of aluminum films on silicon substrates. However, at indentation depths approaching the film thickness, where the hydrostatic pressure becomes great enough to deform the substrate, their model fails. As the indenter-substrate spacing (h) approaches zero, the predicted hardness goes to infinity. This type of model also fails once the indenter passes through the film into the substrate. Therefore, in order to predict hardness at indentation depths greater than the film thickness, a two stage model has been developed.

The two stage model builds on equation 4 by incorporating substrate contributions to the measured hardness on a weighted area basis. The equation for measured hardness as a function of depth of penetration can therefore be written as:

$$H_m = \frac{H_f A_f (1 + \beta (\frac{r_o - r}{h})) + H_s A_s}{A_f + A_s} \quad (5)$$

where H_s is the substrate hardness, A_s is the projected area of the indenter in the substrate, and A_f is the projected area of the indenter in the film. Therefore, $A_s + A_f$ should equal the projected area of the indenter.

In order to differentiate between substrate and film contributions to the measured hardness, the indenter was sliced into several pieces and the values of r and h for each of these pieces as a function of penetration depth were calculated. In this way the material under each indenter piece can be evaluated separately and summed to compute the film and substrate hardness contributions to the composite hardness.

In this model the portion of the indenter which has penetrated into the film was cut into twenty equally spaced slices. The radius, distance from the substrate and projected area under each slice as a function of depth of penetration were calculated for each slice, as shown in Figure 2. The radius of the indent at the film surface is r_o . The values of r_o , r , h and area under each slice depend on the shape of the indenter and the depth of penetration. Therefore, the area function of the indenter must be known. We have modelled the indenter as a conical diamond with the same area function as that which had been experimentally determined for the Berkovich diamond indenter used.⁴ It should be noted that the volume of material under the first slice (or tip of the indenter) is a solid cylinder, while the volume under the rest of the slices is a tube. It is the cross sectional area of the tube (or cylinder) under the slice which is used as the area of the slice in the calculation. Summing the areas under each slice would therefore result in the total projected area of the indenter.

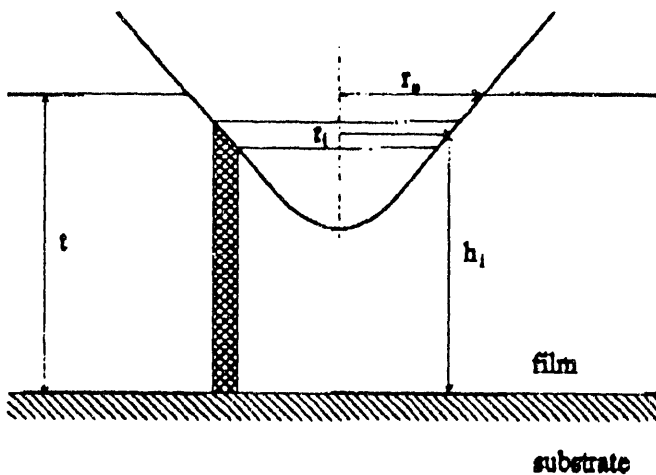


Figure 2. Schematic of indenter showing dimension used for each slice in equation 5.

As the depth of penetration increases, the model evaluates the constrained hardness of the film under each slice, using the frictional constraints in equation 4. As each slice approaches the substrate, the predicted constrained hardness of the film under that slice becomes greater than that of the substrate. However, this does not make physical sense, as once the material under that area becomes constrained enough to be as hard as the substrate, then the substrate will start to deform. Therefore, the maximum allowable constrained hardness of the film is set to that of the substrate. That a film can become as hard as the substrate has been observed by Engel and Roshon,⁸ where a soft film was seen to penetrate into a hard substrate. Using this two stage area approach, indentation depths greater than the film thickness were able to be modelled.

Results/Discussion

Using H_f and β as adjustable parameters, equation 5 was fit to two sets of experimentally determined hardness versus depth curves, for titanium and Ta_2O_5 films on sapphire. The hardness versus depth experiments were performed as described in Fabes *et al.*⁴ A substrate hardness of 35 GPa was used for both sets of data. The resulting curve fits are shown as the solid lines in Figures 3 and 4 for the titanium and Ta_2O_5 films, respectively. The resulting parameters determined for the films are given in Table I. The calculated hardness values for the titanium films decrease from 9.7 GPa for the thinnest film to 8 GPa for the thickest film. The frictional parameter, β , decreases from a value of 0.335 for the thinnest film to 0.005 for the thickest. The parameters for the Ta_2O_5 films follow a similar trend. Hardness values decrease from 9.6 to 7.1 GPa, and β decreases from 0.45 to 0.16, as thickness increases.

Table I: Curve fit parameters for titanium and Ta_2O_5 coatings on sapphire determined using two stage area model.

Titanium			Ta_2O_5		
Thickness (nm)	Hardness (GPa)	β	Thickness (nm)	Hardness (GPa)	β
75	9.7 \pm 0.11	0.335 \pm 0.01	100	9.6 \pm 0.26	0.45 \pm 0.043
105	9.6 \pm 0.06	0.16 \pm 0.004	115	8.3 \pm 0.20	0.18 \pm 0.017
135	9.4 \pm 0.06	0.056 \pm 0.004	160	7.1 \pm 0.11	0.16 \pm 0.014
165	8.5 \pm 0.10	0.045 \pm 0.005	100C	9.6 \pm 0.26	0.03 \pm 0.015
195	8.5 \pm 0.05	0.023 \pm 0.001			
250	8.0 \pm 0.05	0.005 \pm 0.001			

It was anticipated that the value of β should remain constant for all film thicknesses in a given film/substrate system. As defined in this model, β is a measure of the shear strength at the film/substrate interface. As the titanium film was grown epitaxially with a continuous thickness variation across a single sapphire substrate,⁴ it was expected that the adhesion between the film and substrate should be the same for all of the thicknesses tested. The Ta_2O_5 film was also produced as a film with a continuous thickness variation across a single substrate. However, β decreases as the thickness of the films increase. While there may be some physical basis for a decrease in adhesion as film thickness increase, it was not expected that β should decrease as much as it did. The reason for this is not currently known, although we feel that it is due to the details of the stress state in the film and the geometry of the slices and not due to the analysis used in the development of the model itself.

While the actual value of β for a given film thickness may not yet be accurately determined, the model does result in a lower predicted value of β for films with a reduced film/substrate interfacial strength. This can be seen in Figure 5, which shows 100 nm Ta_2O_5 films on sapphire with and without a carbon layer between the film and substrate. The fitted parameters for the film with a carbon layer are given in Table I, as film 100C. The film hardness was 9.6 GPa in both cases, but β was reduced from 0.45 for the film without carbon to 0.03 for the film with a carbon undercoat.

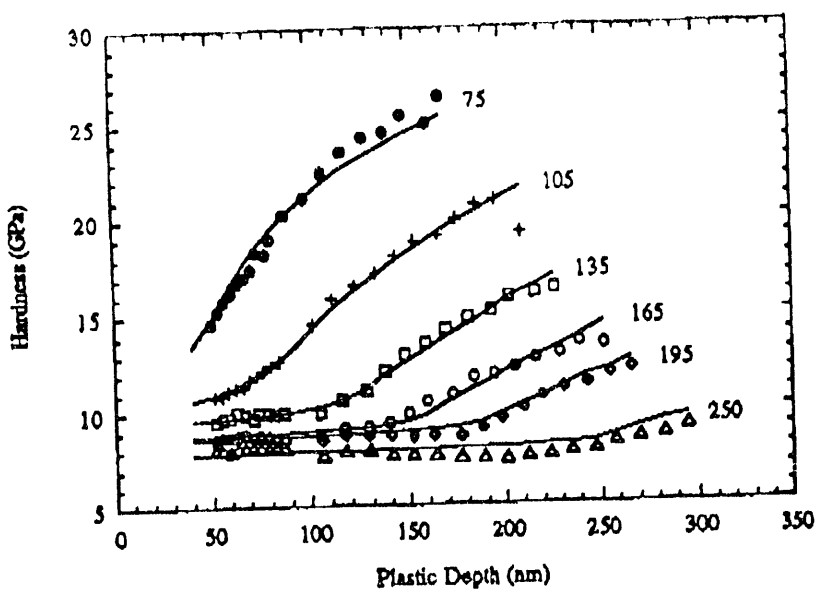


Figure 3. Hardness versus depth for titanium films on sapphire.
 Solid lines correspond to fit of two stage area model,
 using H_1 and β as adjustable parameters. Numbers next
 to each data set are film thickness.

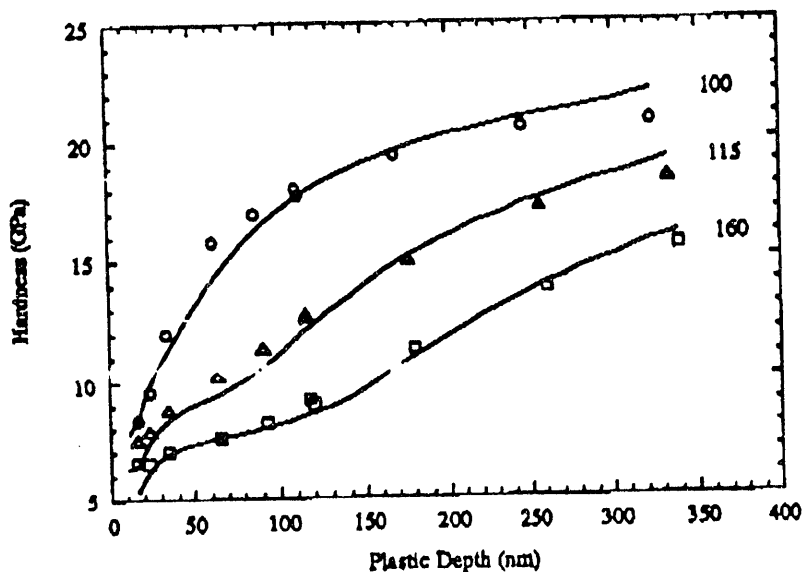


Figure 4. Hardness versus depth for Ta_2O_5 films on sapphire.
 Solid lines correspond to fit of two stage area model,
 using H_1 and β as adjustable parameters. Numbers next
 to each data set are film thickness.

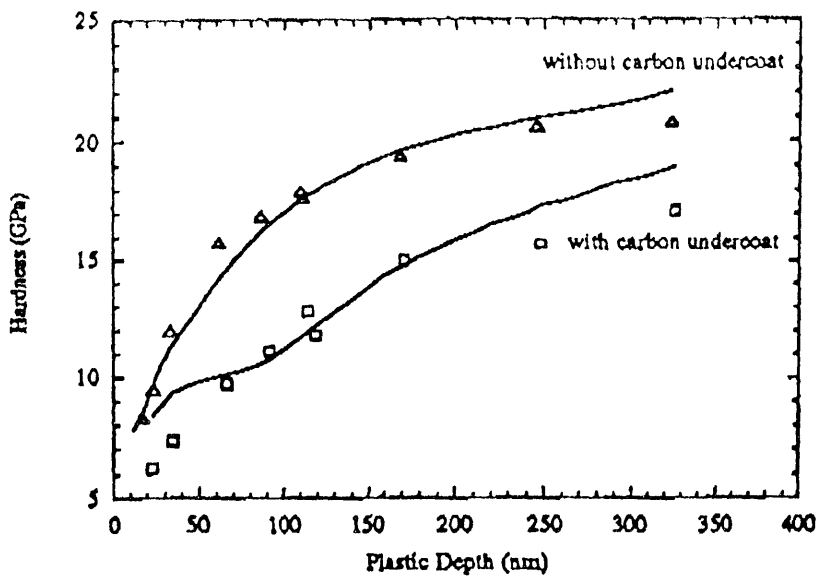


Figure 5. Hardness versus depth for 100 nm Ta_2O_5 films on sapphire, with and without a carbon layer between the film and substrate. Solid lines correspond to two stage area model.

Conclusions

The two stage area model developed here was able to describe experimentally determined hardness versus depth curves for indentation depths both less than and greater than the film thickness. The model considers the film hardness to be an intrinsic value which is modified by constraints due to the adhesion of the film to the substrate. The model uses the film thickness, substrate hardness and area function of the indenter to calculate the predicted composite hardness. The film hardness values calculated by the model are relatively insensitive to film thickness, though the value of β decreases as the film thickness increases in a given film/substrate system. However, for a given film thickness, the model does predict a reduction in β for films which have a reduced film/substrate interfacial strength. It is not known why this occurs, though we feel that it is due to the details of the geometry of slices and the stress state in the material under the indenter. We are currently working on changing the constraint to account for this.

Acknowledgements

Research sponsored in part by the Division of Materials Science, U.S. Department of Energy, under contract DE-AC05-84OR21400 with Martin Marietta Energy Systems, Inc., and through the SHaRE Program, under contract DE-AC05-76OR00033 with Oak Ridge Associated Universities.

References

1. A.K. Bhattacharya and W.D. Nix, International Journal of Solids and Structures, **24** [12], 1287-1298 (1988).
2. P.M. Sargent, in Microindentation Techniques in Materials Science and Engineering, edited by P.J. Blau and B.R. Lawn (American Society of Testing and Materials, Philadelphia, PA, 1986).
3. P.J. Burnett and D.S. Rickerby, Thin Solid Films, **148**, 41-50 (1987).
4. B.D. Fabes, W.C. Oliver, R.A. McKee and F.J. Walker, Journal of Materials Research, **7** [11], 3056-3064 (1992).
5. B. Jonnson and S. Hogmark, Thin Solid Films, **114**, 257-269 (1984).
6. D. Stone, W. LaFontaine, P. Alexopoulos, T. Wu and C. Li, Journal of Materials Research, **3** [1], 141-147 (1988).
7. G.E. Dieter, Mechanized Metallurgy (McGraw-Hill, New York, 1986), 3rd edition.
8. P.A. Engel and D.D. Roshon, Journal of Adhesion, **10**, 237 (1979).

-253

DISCLAIMER

This report was prepared as an account of work sponsored by an agency of the United States Government. Neither the United States Government nor any agency thereof, nor any of their employees, makes any warranty, express or implied, or assumes any legal liability or responsibility for the accuracy, completeness, or usefulness of any information, apparatus, product, or process disclosed, or represents that its use would not infringe privately owned rights. Reference herein to any specific commercial product, process, or service by trade name, trademark, manufacturer, or otherwise does not necessarily constitute or imply its endorsement, recommendation, or favoring by the United States Government or any agency thereof. The views and opinions of authors expressed herein do not necessarily state or reflect those of the United States Government or any agency thereof.

DATE
FILMED

11 / 19 / 93

END

